Electronic Supplementary Material (ESI) for Inorganic Chemistry Frontiers.

Supporting Information

Portable Self-powered Photoelectrochemical Immunosensor Based on Cu_3SnS_4 Nanoflower for Ultra-sensitive and Real-time Detection of Human Cytochrome *c*

Xin Zhang[a], Ling-Hua Jin[a], Yan-Yan Li[b], Zi-Zhen Xiao[a], Yu Feng[b], Ying-Wu Lin[b]*, and Ye Zhang[a]*

a. Lab of Optoelectronic Technology for Low Dimensional Nanomaterials, School of Chemistry and Chemical Engineering, University of South China, Hengyang 421001, China
E-mail: **yezhang@usc.edu.cn**
b. Key Lab of Protein Structure and Function of Universities in Hunan Province, School of Chemistry and Chemical Engineering, University of South China, Hengyang 421001, China
E-mail: **ywlin@usc.edu.cn**

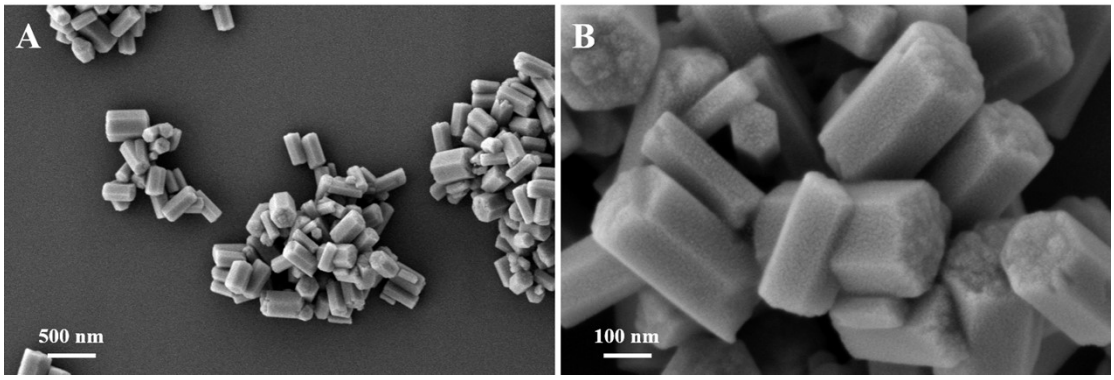

Figure S1. (**A**) SEM image of $CuSn(OH)_6$ (500 nm) and (**B**) SEM image of $CuSn(OH)_6$ (100 nm).

X-ray diffraction (XRD) was employed to analyze the purity and crystal structure of the products. As indicated in **Figure S2**, $CuSn(OH)_6$ is a tetragonal sulfide with five strong peaks located at 2θ positions of 12.5°, 21.8°, 25.2°, 29.7°, 32.4°, 33.5°, 39.3°, 44.4°, 45.4°, 49.1°,51.7°, 54.3°, 60.8°, 67.7° and 78.3°, corresponding to diffractions from the (100), (110), (200), (201), (102), (210), (202), (220), (212), (103), (400), (203), (410), (204) and (332) planes of the $CuSn(OH)_6$ crystal, which is consistent with the description in the literature[1, 2].

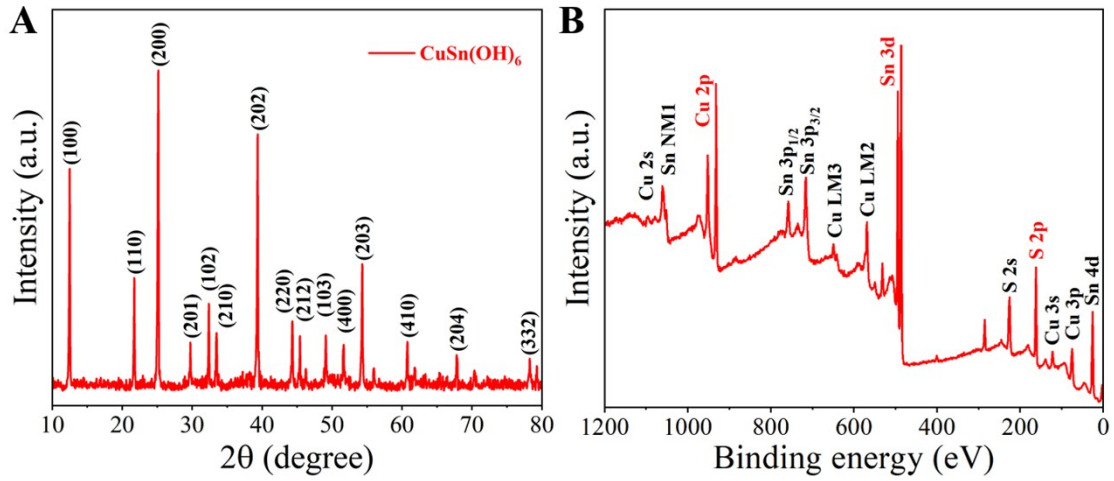

Figure S2. (**A**) XRD patterns of $CuSn(OH)_6$; (**B**) XPS spectra of Cu_3SnS_4.

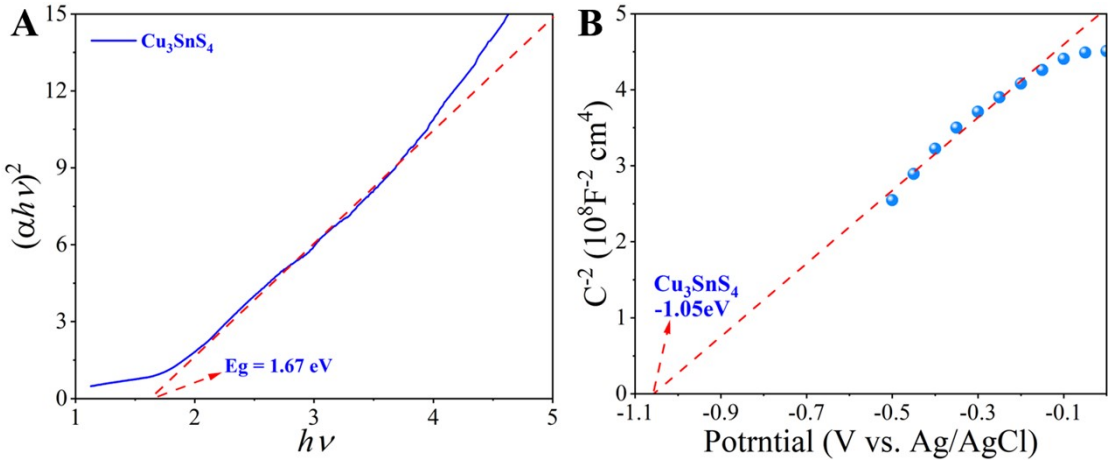

Figure S3. (**A**) Plots of $(\alpha h\nu)^2$ vs. $(h\nu)$ used to evaluate the optical bandgaps of Cu_3SnS_4; (**B**) Mott-Schottky curves of Cu_3SnS_4.

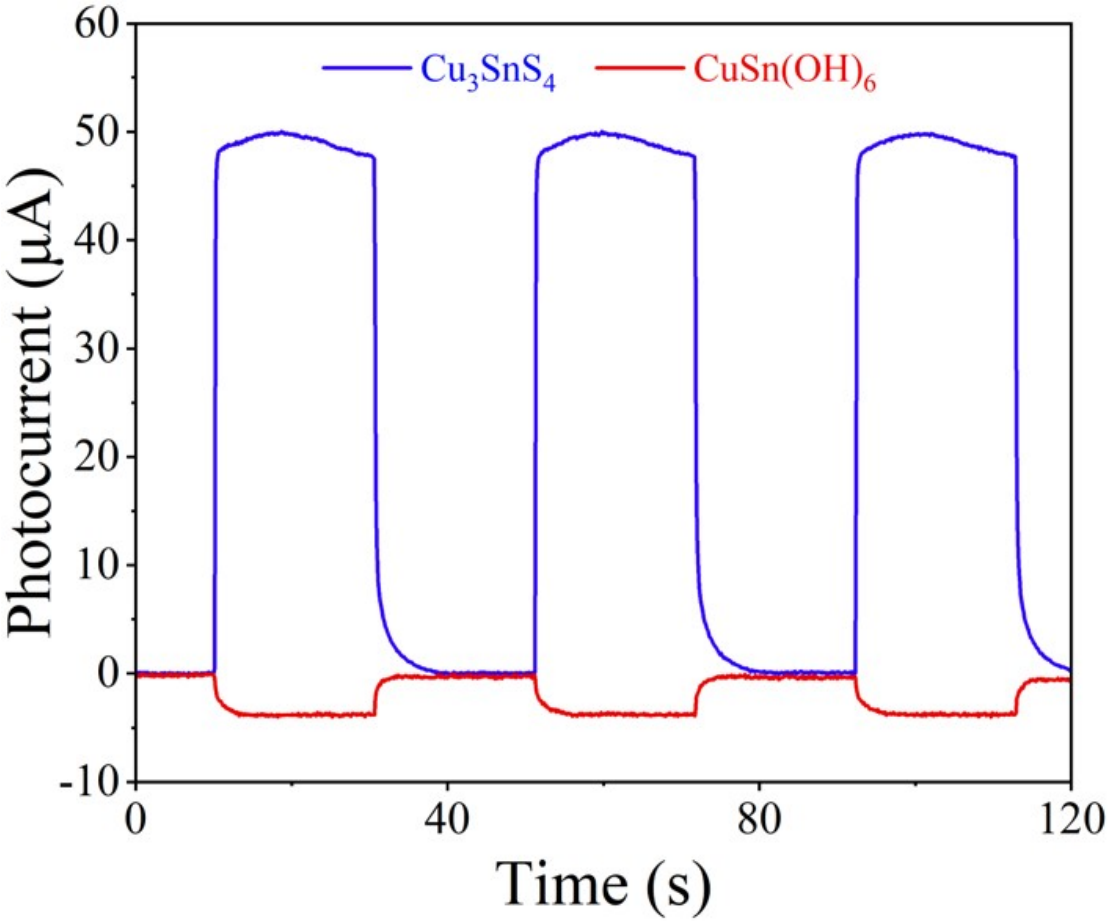

Figure S4. Photocurrent response of electrodes of different materials.

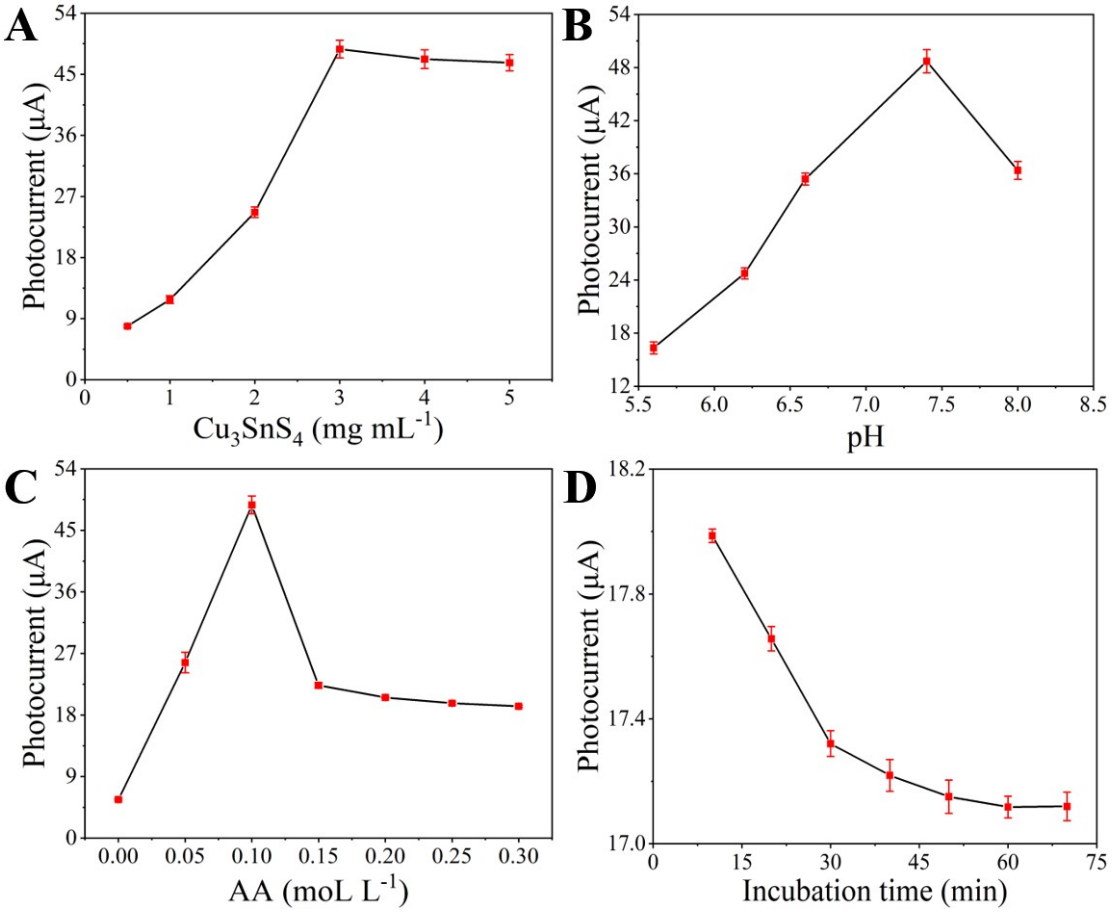

Figure S5. Effects of (**A**) the concentration of Cu_3SnS_4; (**B**) the pH value of the PBS; (**C**) the concentration of AA; (**D**) the incubation time of Cyt *c*.

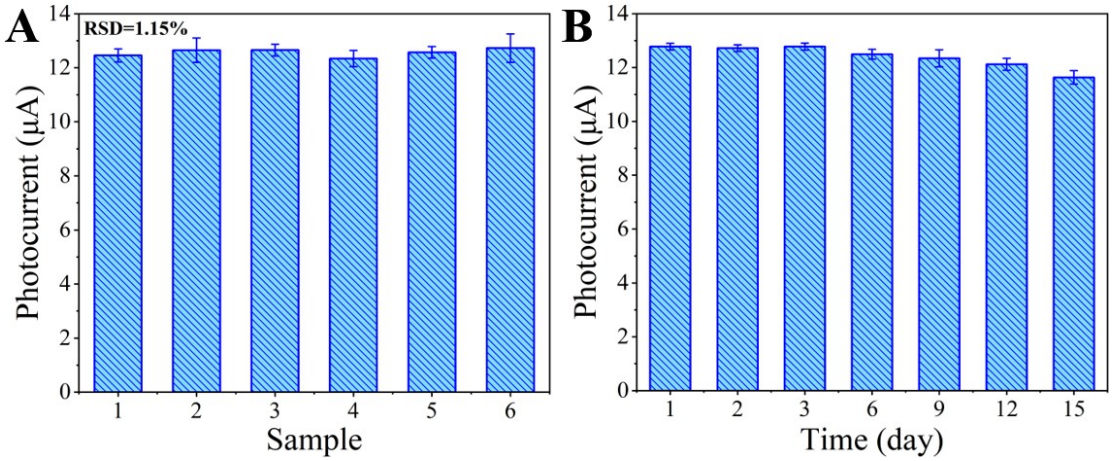

Figure S6. (**A**) Reproducibility (Cyt *c*: 100 pM) and (**B**) Storage stability of the PEC immunosensor.

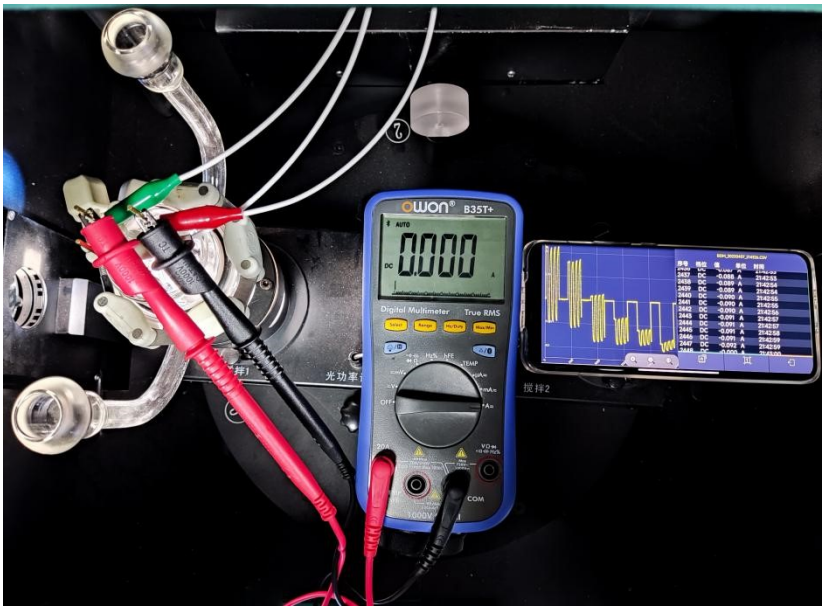

Figure S7. Real-time detection of Cyt *c* system.

Table S1 Simulation parameters of the equivalent circuit components

Electrode	R_s (Ω)	R_{et} (Ω)	*I*
Cu_3SnS_4	22.86	22.13	49.8μA
Cu_3SnS_4/CS	23.53	42.08	35.6μA
Cu_3SnS_4/CS/anti-Cyt *c*	23.97	68.29	28.8μA
Cu_3SnS_4/CS/anti-Cyt *c*/BSA	23.70	79.75	19.6μA
Cu_3SnS_4/CS/anti-Cyt *c*/BSA/Cyt *c*	23.30	97.00	12.6μA

Table S2 Different Cyt *c* detection methods were compared

Method	Nanomaterials	Linear range	Detection limit	References
Fluorescence	CdTe	0.5 μM-2.5 μM	0.5 μM	[3]
Fluorescence	VS_2-Nanosheet	0.75 nM-50 nM	0.5 nM	[4]

Fluorescence	DNA-AgNCs@tween 80	0.8 nM-20000 nM	0.8 nM	[5]
Colorimetric, chemiluminescence	β-$Co(OH)_2$ CMk	1 pM-5 μM, 50 μM-1 mM	2 fM	[6]
EIS	Cyt-c/Polypyrrole/SPE	10 pM-1 nM	5 pM	[7]
EIS	CdS/graphene	1 nM-100 nM	0.3 nM	[8]
PEC	$CdS/CuInS_2/Au/TiO_2$	5 pM-100 nM	5 pM	[9]
PEC	**Cu_3SnS_4**	**1 fM-1000 nM**	**0.35 fM**	**This work**

Table S3. Analytical results of Cyt *c* in human serum samples

Sample	Added (nM)	Detection content (nM, n=3)	Average content (nM)	RSD (%)	Recovery (%)
Serum #789	0.1	0.085、 0.095、 0.108	0.096	1.55	96.17
Serum #757	0.1	0.085、 0.116、 0.92	0.098	1.89	97.63
Serum #730	0.5	0.465、 0.554、 0.486	0.502	3.64	100.4
Serum #729	1	1.065、 0.851、 0.956	0.958	1.34	95.76

References:

1. J. Huang, X. Xu, C. Gu, S. Yao, Y. Sun and J. Liu, Large-Scale Selective Preparation of Porous SnO_2 3D Architectures and Their Gas-Sensing Property, *CrystEngComm*, 2012, **14**.
2. J. Huang, Y. Wang, C. Gu and M. Zhai, Large Scale Synthesis of Uniform CuS Nanotubes by a Sacrificial Templating Method and Their Application as an Efficient Photocatalyst, *Materials Letters*, 2013, **99**, 31-34.
3. R. M. Amin, S. A. Elfeky, T. Verwanger and B. Krammer, Fluorescence-based CdTe Nanosensor for Sensitive Detection of Cytochrome *C*, *Biosens. Bioelectron.*, 2017, **98**, 415-420.
4. X. Yin, J. Cai, H. Feng, Z. Wu, J. Zou and Q. Cai, A VS_2/Aptamer-Based Cytochrome *c* Sensor was Successfully Constructed by First Applying the DNA-Adsorbing Ability/Fluorescence-Quenching Properties of VS_2 in Bioanalysis., *New J. Chem.*, 2014.
5. Y. Qin, M. Daniyal, W. Wang, Y. Jian, W. Yang, Y. Qiu, C. Tong, W. Wang and B. Liu, An Enhanced Silver Nanocluster System for Cytochrome *c* Detection and Natural Drug Screening Targeted for Cytochrome *c*, *Sens. Actuators B Chem*, 2019, **291**, 485-492.

6. F. Mesgari, S. M. Beigi, N. Fakhri, M. Hosseini, M. Aghazadeh and M. R. Ganjali, Paper-Based Chemiluminescence and Colorimetric Detection of Cytochrome *c* by Cobalt Hydroxide Decorated Mesoporous Carbon, *Microchemical Journal*, 2020, **157**.
7. Q. Wen, X. Zhang, J. Cai and P. H. Yang, A Novel Strategy for Real-Time and in Situ Detection of Cytochrome *c* and Caspase-9 in Hela Cells During Apoptosis, *Analyst*, 2014, **139**, 2499-2506.
8. Y.-P. Dong, J. Wang, Y. Peng and J.-J. Zhu, Electrogenerated Chemiluminescence Resonance Energy Transfer Between Luminol and CdS/Graphene Nanocomposites and its Sensing Application, *Journal of Electroanalytical Chemistry*, 2016, **781**, 109-113.
9. L. Wang, W. Gu, P. Sheng, Z. Zhang, B. Zhang and Q. Cai, A label-free Cytochrome *c* Photoelectrochemical Aptasensor Based on $CdS/CuInS_2/Au/TiO_2$ Nanotubes, *Sens. Actuators B Chem*, 2019, **281**, 1088-1096.